Kufa Journal of Engineering
Vol. 10, No. 1, January 2019, P.P. 127-139
Received 11 February 2018, accepted 25 March 2018

COMPARATIVE ANALYSIS OF ATOMIZING SPRAY FROM DIESEL INJECTORS USING ALGAE AND BIODIESEL FUELS

Noor M. Jasim[1]

[1] Mechanical Engineering Department, College of Engineering University of Kufa, Iraq.
Email: Noorm.alhasnawi@uokufa.edu.iq

http://dx.doi.org/10.30572/2018/kje/100110

ABSTRACT

Fuel atomization in diesel compression ignition engines is significantly affected on the performance, evaporation, self-ignition, and emissions of the engine. Therefore, the quality of the spray atomization has to study at first. Algae-Derived renewable diesel fuel in a single hole nozzle atomizer has been chosen as an alternative fuel for diesel. The differences in physical properties of algae-derived renewable diesel, biodiesels (from palm and cooked oil) and pure diesel are effected on both spray characteristics and the internal nozzle flow. Numerical simulations are presented in this study using Eulerian-Eulerian technique to model the spray-gas interaction. The spray moments model has been used to characterize the spray parameters. First, the model is validated against the spray tip penetration of diesel spray characteristics obtained from the experimental data conducted in house-code using constant volume spray chamber and the results show a good agreement. Then, comparisons were made among the selected fuels. The numerical simulations show that the algae-derived renewable diesel is very similar to pure diesel and can be used as an alternative fuel.

KEYWORDS: Spray modelling, algae fuel, biodiesel fuel, drop number size moments.

1. INTRODUCTION

As Biodiesel fuel, its demand currently continues to increase. Algae is most likely that biodiesel fuel will be an important source in the future of green energy market of the world. Experimental work for several alternative fuels in a twin-fluid airblast atomizer was carried out by Legg et al., 2012, to investigated atomization performance. They observed that the break-up process and velocity fields were approximately similar among the fuels. Also, under evaporation conditions, the rate of evaporation was depended on the fuel volatility. Extinction strain rates of diffusion and premixed flames of petroleum-derived fuels and an algae-derived hydrotreated renewable F-76 diesel fuel were experimentally measured by Li et al., 2013 in the counterflow configuration under reacting conditions of a fuel-containing stream temperature of 443 K and at atmospheric pressure. The results show that the bio-derived fuels have longer extinction strain rates of flames of than petroleum-derived fuels. Experiments were made by Gowdagiri et al., 2014 To determine the ignition delay time for two types of diesel fuels, conventional military-grade F-76 and an alternative hydroprocessed renewable diesel fuel derived from algal oil HRD-76. Experiments showed that at higher temperature both fuel have an indistinguishable ignition delay time. Whereas at lower temperatures, HRD-76 has shorter ignition delay time than F-76. A test on diesel engine by using algae biodiesel was measured by Nagane and Choudhari, 2015, the cetane number of algae biodiesel is higher than of diesel, and the cetane number of algae biodiesel blends can be improved by increasing the blending ratio.

Under high injection pressures in a constant volume combustion chamber, the spray atomization characteristics of heavy fuel oil -microalgal biodiesel were numerically simulated under ambient condition by Ghadimi et al., 2017 using an openfoam code. The CFD analyses were based using three different blended volume percent ages of microalgal biodiesel in comparison with pure heavy fuel oil. From their calculations, the spray tip penetration of microalgal biodiesel was longer than heavy fuel oil. The Sauter mean diameter was lower than heavy fuel oil due to lower fuel properties (density, viscosity, and surface tension). Conventional military diesel fuel was studied by Valco et al., 2017, the spray combustion of F-76, and hydrotreated renewable diesel fuel, HRD-76. The characteristic of HRD-76 was shown to have shorter auto-ignition delays and shorter lift-off lengths as compared with F-76.

In the present paper, hydrotreated renewable diesel fuel HRD-76 has been compared with two biodiesel fuel based on palm and cooking oil and pure diesel of their spray properties characteristics. Spray atomization characterization is numerically simulated using in-house code. A Eulerian-Eulerian framework is implemented in the modeling two-phase flow. The

spray moments theory is used to represent spray parameters which include spray tip penetration, Sauter means diameter and spray area.

2. MATHEMATICAL MODEL AND CONSIDERATIONS

A two-dimensional unsteady Eulerian-Eulerian framework is suggested to simulate the gas-liquid two-phase flow behavior. In this approach, both phases are considered as interacting and inter-penetrating as a continuum. In the Eulerian approach, the dispersed droplet dynamics are described by transporting the Population Balance Equation (PBE). Due to the interacting with the continuous gas phase the extra source term in the transport equation for the volume-specific drop size number density function f(D) written as (Dems, 2015):

$$\frac{\partial f(D)}{\partial t} + \frac{\partial}{\partial x}\left(Uf(D)\right) = S \qquad 1$$

Where S is the interacting source terms with the gas phase, and U is the liquid velocity. The k-th moment of the drop number density function f (D) is determined by:

$$M^{(k)} = \int_0^\infty D^k f(D)\, dD \qquad 2$$

From this definition permits for a physical interpretation of different order moments. Particularly, the fourth order of moment represents the association with the disperse phase volume fraction $\alpha = \frac{\pi}{6} M^3$. From this point, it can be used to switch with the Eulerian equations for the dispersed phase to the proposed transport equations for the moments. Representative local droplet diameters are defined by evaluating moment relations (for example Sauter Mean Diameter SMD D32= $\frac{M^3}{M^2}$). The transport equations for the moments are formulated with an individual velocity related to the moment transport velocities $u(k)$ as:

$$\frac{\partial M^{(k)}}{\partial t} + \frac{\partial}{\partial x}\left(U^{(k)} M^{(k)}\right) = S^k \qquad 3$$

The moment-average velocity U, of the k − th component of droplet velocities U averaged over the k − th moment $M^{(k)}$ is defined as

$$U = \frac{\int_0^\infty D^{(k)} U^{(k)} f(D) dD}{M^k} \qquad 4$$

The moment's method is presented in this approach based on the droplet number size distribution, f(D), is defined as a multiple of the droplet number probability distribution of droplet radius as below

$$f(D) = \int_{Dmin}^{Dmax} F(D)\, dD \quad (5)$$

Where F(D) is the droplet number probability distribution. The general gamma number size distribution is proposed here by

$$f(D) = M^{(0)} \frac{(k+2)^k}{\Gamma(k) D_{32}} D^{k-1} e^{-(k-2)D/D32} \quad (6)$$

And

$$\Gamma(k) = \int_0^{\infty} x^{k-1}\, e^{-x}\, dx \quad (7)$$

Where Γ(k) is the gamma function and D32 is the Sauter mean diameter of the number size distribution of the drops. This is defined by D32 = M(3)/M(2).

$$M_{pq}^{p-q} = \frac{2^{p-q}\, M_p}{M_q} \quad (8)$$

For numerical calculations, the gamma function can be approximated by Windschitl, 2018:

$$\Gamma(k) = \left[\left(\frac{k}{e} \left(k * \sinh\left(\frac{1}{k} + \frac{1}{810 k^6} \right) \right)^{1/2} \right)^k \right] \left(\frac{2\pi}{k} \right)^{1/2} \quad (9)$$

The gas phase transport equations employed here takes the standard form of:

$$\frac{\partial}{\partial t}\left(\rho_g \Theta\right) + \frac{\partial}{\partial x_j}\left(\rho_g \Theta U_{gj}\right) = -S \quad (10)$$

Where Θ is a liquid-volume fraction and S is the source term transported from the liquid phase to the gas phase per unit time within a control volume. The gaseous momentum equation, including turbulence effects, is written as:

$$\frac{\partial}{\partial t}\left(\rho_g \Theta U_{gi}\right) + \frac{\partial}{\partial x_j}\left(\rho_g \Theta U_{gj} U_{gi}\right) - U_{gj}\left[\frac{\partial}{\partial t}\left(\rho_g \Theta\right) + \frac{\partial}{\partial x_j}\left(\rho_g \Theta U_{gj}\right)\right] = \frac{\partial}{\partial t}\left[\mu_{eff}\, \Theta \left(\frac{\partial U_{gi}}{\partial x_j} + \frac{\partial U_{gj}}{\partial x_j}\right)\right] - \Theta \frac{\partial P}{\partial x_i} - \frac{\partial}{\partial x_j}\left[\frac{2}{3}\, \Theta\, \rho_g k \delta_{ij}\right] + S_m\left(U_{li} - U_{gi}\right) + S_{Ui} \quad (11)$$

The effective viscosity, μ_{eff}, is given by

$$\mu_{eff} = \mu_{lam} + \rho_g C_\mu \frac{k^2}{\epsilon} \quad 12$$

Where k and ϵ are the turbulence kinetic energy and its dissipation rate. The $k-\epsilon$ two-equation model turbulence model is employed in this work (Launder and Spalding, 1972).

3. NUMERICAL METHOD

The transported equations for the gas and liquid phases are coupled, and however, a nonlinear iterative method is needed. The non-linear iterative method is casting these equations into a matrix with a nominally non-linear form with coefficients calculated from the previous iteration values for these variables. The generated matrix from nominally non-linear algebraic equations for continuity and momentum for the gas phase and four moment equations and their momentum is then solved by using (TDMA) algorithm. The line-by-line method used for all the variables an inertial under-relaxation coefficient in order to accelerate convergence. The simple algorithm for pressure/velocity coupling.

4. RESULTS AND DISCUSSION

Four test cases are considered here for a non-evaporative solid cone spray of different fuels. All fuel properties are taken from (Legg et al., 2012; Launder and Spalding, 1972) and are listed in Table 1. For validation aims the spray moments model has been used to the numerical tests, Fig. 1 shows a comparison between the test case with experimental data. All the numerical parameters used for the initial prediction wherever possible are taken from Emekwuru and Watkins (Wang et al., 2010) and presented in Table 2. The comparison shows that the model has the same trend. It can be observed that the model agrees with the experimental work of other researchers which can give the opportunity to investigate the behavior other biodiesel fuels. Fig. 2 shows another comparison for the spray tip penetration of different fuels at injection pressure 9.9 MPa. The development of spray penetration for the test cases of the selected fuels at ambient pressure explained that the spray tip penetration in the case of algae-derived HRD-76 fuel has longer penetration than other BDFp, BDFc, and diesel fuel and it is the closest to the experimental data. Not only the spray penetration is the crucial parameter during the atomizing process, however from the numerical simulation for the tests cases the third moment (liquid volume fraction) has been chosen to show the shape for the injected fuel.

Fig. 3 shows the configuration for each fuel, from these plots, it can be observed that algae-derived HRD-76 has a similar shape to the diesel fuel because they have approximately the same level of density. BDFp and BDFc have similar shape due to the same reason. Fig. 4 shows the proposed gamma distribution in order to represent the distribution of droplets during the injection period. This Fig.has been placed to illustrate to the reader the shape of the drop size distribution behavior. Fig. 5 shows the sum of the total droplets radii (M1) along the axial distance downstream from the injector orifice. The concentration of this moment is remarkably decreased with the increase of axial distance due to the spray dispersion process. From the distribution and for the main reason for this trend algae-derived HRD-76 has improved in fuel atomization that diesel, BDFp, and BDFc. This due to lower surface tension property. Especially, it represents an important parameter in the disintegration process. This parameter is the Weber number,

$$W_e = \frac{\rho U^2 d}{\sigma} \qquad 13$$

In order to get a fully understand for the above investigation, the distribution of the liquid volume fraction (M3) in the axial direction and radial directions are chosen to illustrate the way in which the liquid droplets are spread out. Figs. 6 and 7 again shows that algae-derived HRD-76 has a higher rate of consternation due to atomization processes than other fuels. The Sauter mean diameter D32, which is defined as the ratio of the total liquid volume to the total droplet surface area in a spray, is average droplet diameter used for representing the spray. Fig. 8 shows contour plots for the Sauter mean radius. Fig. 8a shows a comparison of Sauter mean radius SMR between algae-derived HRD-76 and diesel, and it can be noticed that there is a slightly different from diesel. Similarly, Fig. 8b shows the comparison of SMR between BDFp and BDFc. Both are considered as heavy fuel because their density is high compared with diesel fuel. Fig. 8c compared SMR between algae-derived HRD-76 and BDFp, where a lower level of values for algae-derived HRD-76 because is considered as a promising lighter fuel than BDFp. It showed be noticed that these comparisons are at time of (2.00 msec). The differences between these plots are very small due to the spray development (at the end of injection period). Fig. 9 shows the axial variation of SMR from the injector. Therefore the droplets size at the front of the spray is high that gives an indication that there are small droplets area because of low injection velocity.

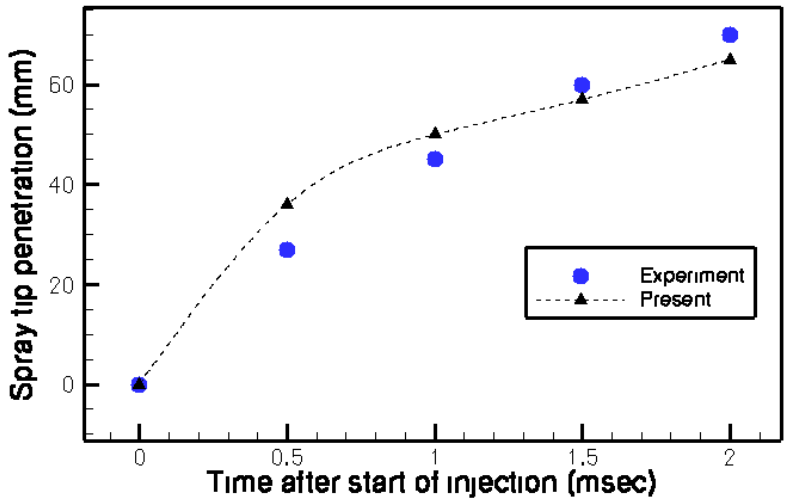

Fig. 1. Validation of numerical model vs. experimental data (Wang et al., 2010).

Table 1. Fuel properties and composition (Legg et al., 2012; Launder and Spalding, 1972).

Fuel type	Diesel	Algae HRD/F-76	BDFp	BDFc
Density (288 K)(kg/m^3)	830	811.1	874.4	885.1
Viscosity (303 K) (mm^2/s)	3.36	3.699	5.53	4.45
Surface tension (mN/m)	25.5	27.7	26.2	25.7

Table 2. Experimental conditions for the data of Hiroyasu and Kadota (Wang et al., 2010).

Parameter	Numerical value
Ambient Pressure (MPa)	1.1
Spray Angle (degree)	10
Injection Velocity (m/s)	102.0
Drop SMR at 65mm (μm)	21.2
Injection Pressure (MPa)	9.9
Nozzle Radius (mm)	0.15
Chamber radius(m)	0.037
Chamber axial length (m)	0.2

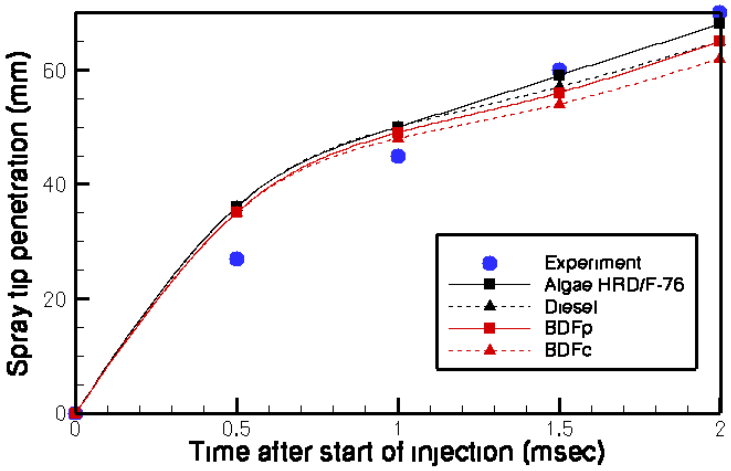

Fig. 2. Comparison of numerical model vs experimental spray tip penetration for different fuels at injection pressure of 9.9 Mpa (Wang et al., 2010).

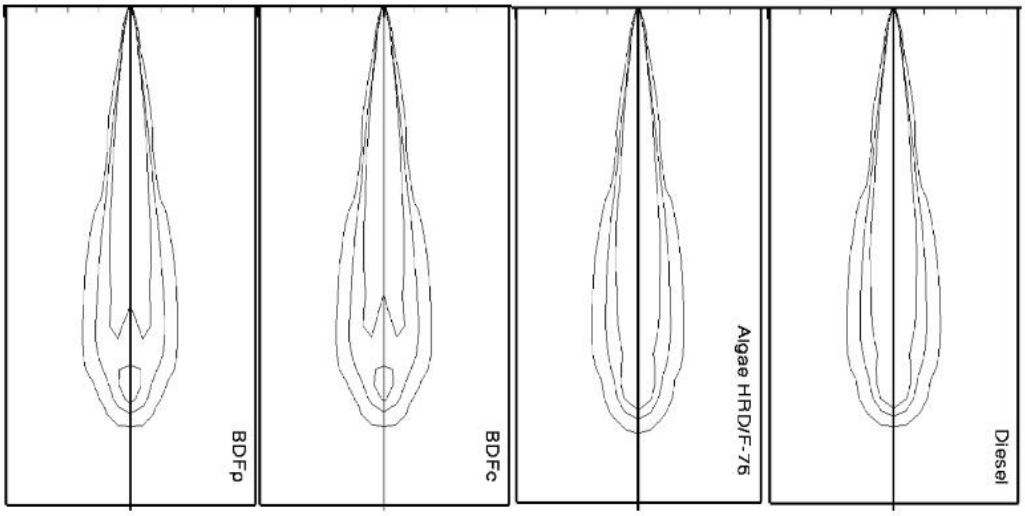

Fig. 3. Spray volume of fraction structure of different fuels at 2.00 msec.

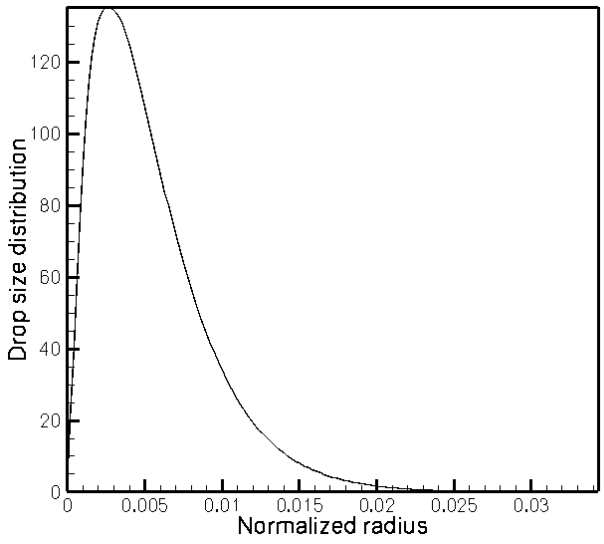

Fig. 4. Proposed gamma drop size distribution function.

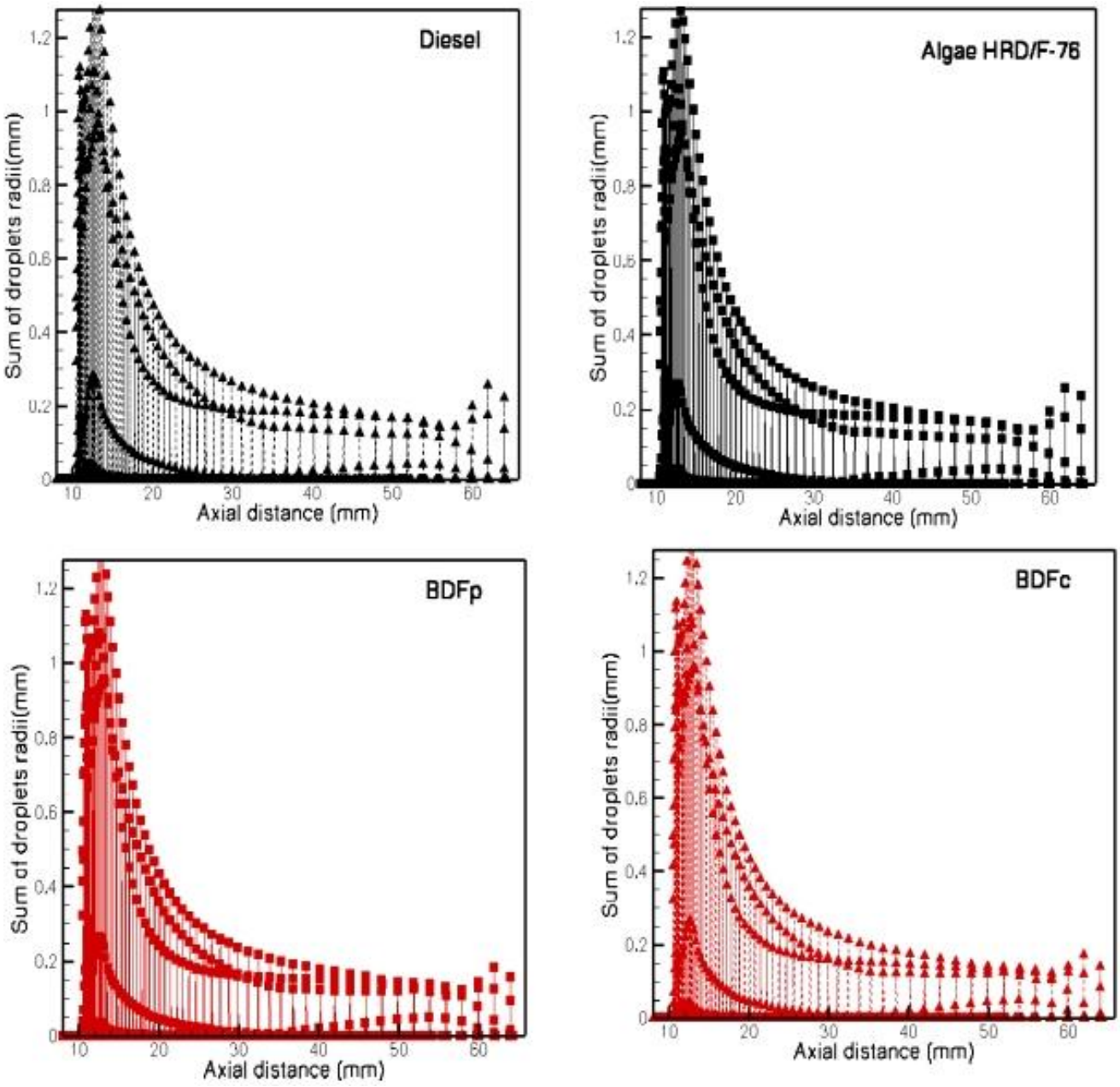

Fig. 5. Comparison of distribution of sum of drop radii of different fuels along the axial distance.

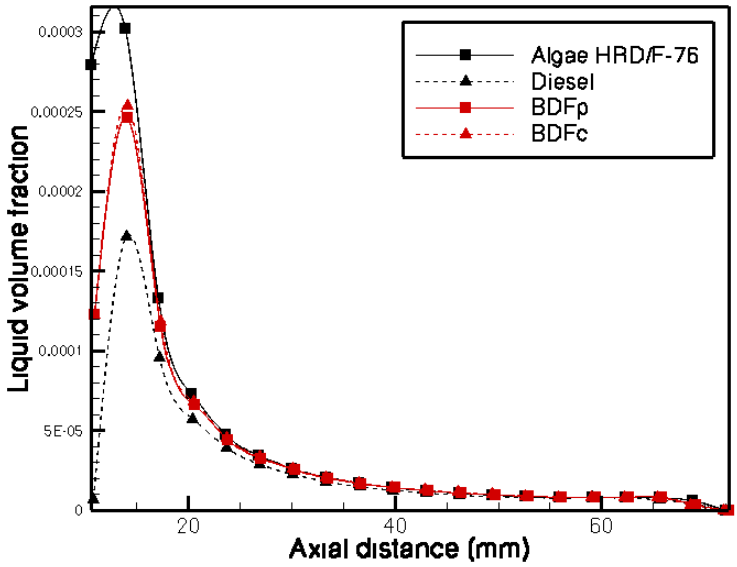

Fig. 6. Axial profile of spray liquid volume of fraction along axial distance for different fuels.

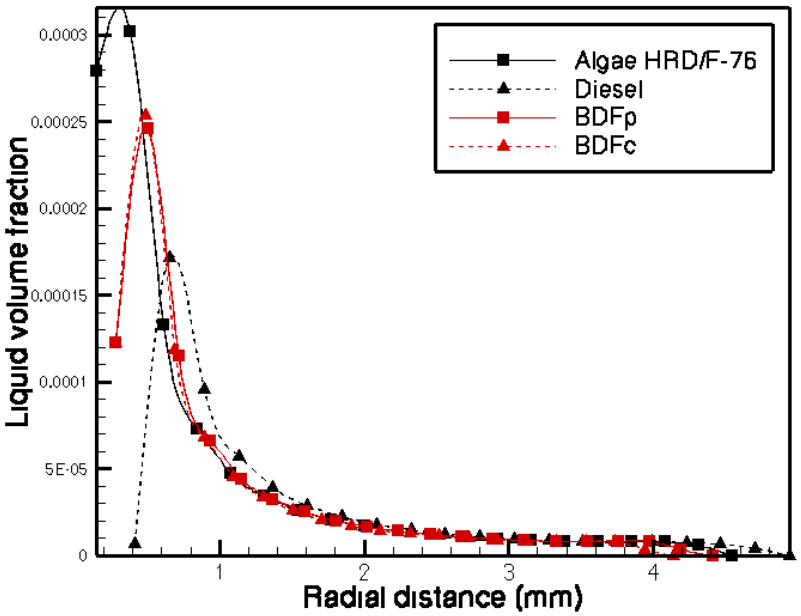

Fig. 7. Radial profile of spray liquid volume of fraction along radial distance for different fuels.

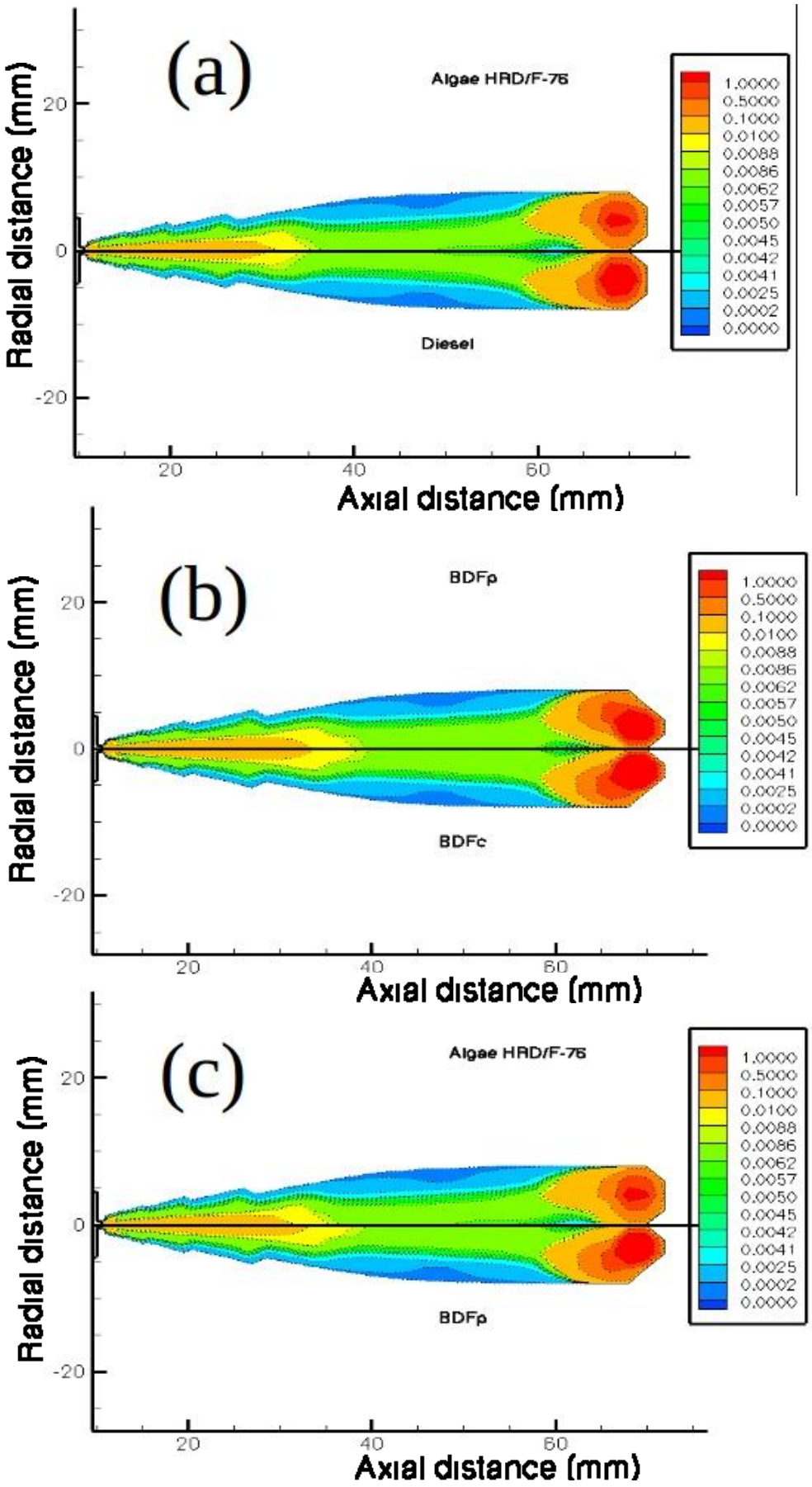

Fig. 8. Comparison among contour plots of Sauter mean diameter of different fuels at 2.00 msec.

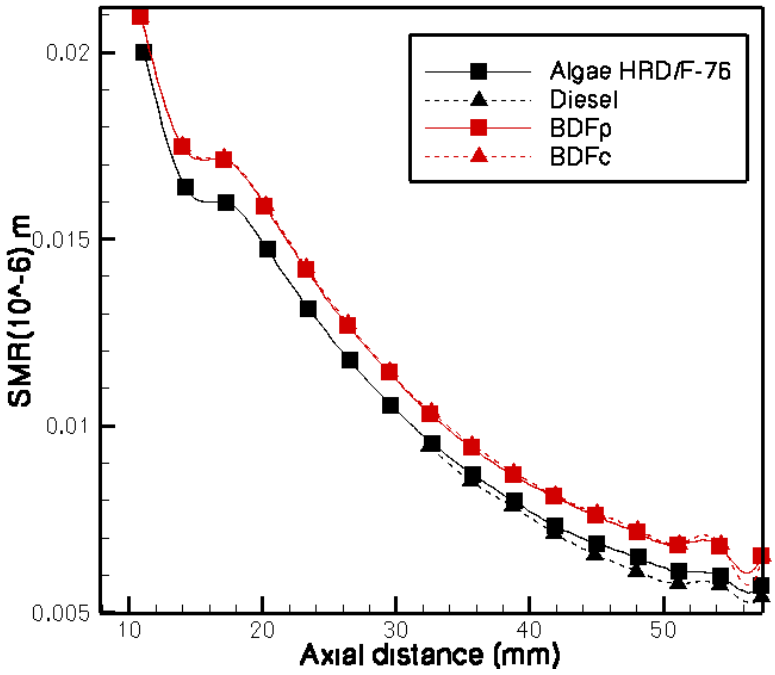

Fig. 9. Axial profile of spray Sauter mean radius along axial distance for different fuels.

5. CONCLUSIONS

Among the most important extracted results that can be found in this work are the followings:

1. It can be observed that algae-derived HRD-76 has a similar shape to the diesel fuel because they have approximately the same level of density.

2. Algae-derived HRD-76 has a higher rate of consternation due to atomization processes than other fuels.

3. It can be noticed that algae-derived HRD-76 has a lower value of Sauter mean diameter at the end front of the spray because there are small droplets can be found and low injection velocity.

6. REFERENCES

Bo Li, Ning Liu, Runhua Zhao, and Fokion N. Egolfopoulos. Extinction Studies of Flames of Heavy Neat Hydrocarbons and Practical Fuels. Journal of Propulsion And Power, Vol. 29, No. 2, March 2013.

Daniel J. Valco, Michael J. Tess, Jacob E. Temme, Matthew S. Kurman, Anna Oldani, Chol-Bum M. Kweon, Matthew A. Oehlschlaeger, Tonghun Lee. Ignition characterization of F-76 and algae-derived HRD-76 at elevated temperatures and pressures. Combustion and Flame 181, 157163, (2017).

Ganesh Nagane, ChandrakishorS. Choudhari. Emission characteristics of diesel engine fueled with algae biodiesel-diesel blends. International Research Journal of Engineering and Technology. Volume: 02 Issue: 04 — July-2015.

Legg J. M., Narvaez A. A., McDonell V. G. Performance of algae-derived renewable diesel in a twin-fluid airblast atomizer. In: Proceedings of the 12th triennial international conference on liquid atomization and spray systems, Heidelberg, Germany (2012).

Nwabueze G. Emekwuru and A. Paul Watkins. Application of moments sprays model to solid cone diesel sprays. SAE 2011-01-1843, (2011).

Parviz Ghadimi, Hashem Nowruzi, Mahdi Yousefifard, Mohammad Feizi Cheka. CFD study on spray characteristics of heavy fuel oil-based microalgae biodiesel blends under ultra-high injection pressures. Meccanica, Volume 52, Issue12, pp 153–170, January 2017.

Patrick Dems. On Eulerian-Eulerian Large Eddy Simulation of Polydispersed, Reacting Spray Flows with Moment Methods. PhD thesis. Technische universität münchen.January 2015

Launder B. E. and Spalding D. B. Mathematical models of turbulence, London academic press, 1972.

Sandeep Gowdagiri, Weijing Wang, Matthew A. Oehlschlaeger. A shock tube ignition delay study of conventional diesel fuel and hydroprocessed renewable diesel fuel from algal oil. Fuel 128, 2129, (2014).

Wang, X., Huang, Z., Kuti, O.A., Zhang, W. and Nishida, K. Experimental and analytical study on biodiesel and diesel spray characteristics under ultra-high injection pressure. International Journal of Heat and Fluid Flow, 31, 659–666, (2010).

Windschitl R. H., http://www.rskey.org/gamma.htm, [accessed on 1/3/2018]